IEEE Access
Multidisciplinary | Rapid Review | Open Access Journal

Received September 2, 2018, accepted September 25, 2018, date of publication October 5, 2018, date of current version October 29, 2018.

Digital Object Identifier 10.1109/ACCESS.2018.2874184

Trajectory Modified in Joint Space for Vibration Suppression of Manipulator

BAOSHI CAO[1], KUI SUN[1], TIAN LI[2], YIKUN GU[1], MINGHE JIN[1], AND HONG LIU[1]
[1]State Key Laboratory of Robotics and System, Harbin Institute of Technology, Harbin 150001, China
[2]Beijing Andawell Science & Technology Co., Ltd., Beijing 100102, China

Corresponding author: Kui Sun (sun.kui@163.com)

This work was supported in part by National Key R&D Program of China under Grant 2017YFB1300400), in part by the Foundation for Innovative Research Groups of the National Natural Science Foundation of China under Grant 51521003, and in part by the National Natural Science Foundation of China under Grant 61603112.

ABSTRACT Trajectory planning method has been proved to be an effective way to suppress robot vibration in multiple experiments, which can be divided into off-line trajectory planning for repetitive task and online trajectory modified for uncertain task. Particle swarm optimization (PSO) is a typical optimization algorithm, which can be used in offline joint trajectory planning, but classical PSO is incapable of optimizing a joint trajectory with variable constraints. Thus, in this paper, a novel compression factor PSO with penalty function named CP-PSO is proposed to modify joint trajectory, thereby achieve minimum residual elastic potential energy in the case of joint angle constraint. However, CP-PSO algorithm still needs plenty of computation time, which is unsuitable for online optimizing uncertain operational task's trajectory. To solve this issue, trajectory modified based on vibration prediction criteria is put forward to suppress manipulator vibration. Particularly, vibration prediction criteria is based on torque error between theoretical joint torque and actual joint torque, as well as the modified trajectory is named as DKA trajectory by the reason of it is composed of three sections, namely, smooth decelerating process, low velocity keeping process, and accelerating process. When vibration is predicted to occur via vibration prediction criteria, DKA trajectory is switched ON to suppress vibration. Finally, experiments are performed on manipulator to verify the proposed methods.

INDEX TERMS Vibration suppression, PSO, penalty function, vibration prediction, trajectory modified.

I. INTRODUCTION

Most light-weight robot joints have elastic elements in drive chain, such as harmonic gear and torque sensor. Above these joints containing elastic elements are named flexible joint, and manipulator with flexible joints is called flexible manipulator. A series of experiments demonstrated that if joint flexibility is neglected in flexible manipulator control, performance of robot motion control will be seriously affected [1]. Furthermore, manipulator vibration caused by joint flexibility, which consists of vibration during joint motion and residual vibration after robot reaching target, is a major factor of manipulator control. Therefore, vibration suppression is a significant topic in flexible manipulator control.

In accordance with distinct principles, suppress robot vibration methods are categorized as passive control, active control, and trajectory planning. Passive control [2]–[7] refers to reduce robot flexibility, which via energy-consuming or energy-storage materials selection, or/and mechanical structure optimization, to suppress robot residual vibration. Moreover, passive control is a simple, effective, widely used approach to suppress manipulator vibration, but it is still constrained by factors, like mechanical structure and materials. Whereas, active control [8]–[17] is suppress robot vibration through a good designed controller, which has a reasonable dynamic response. Furthermore, active control is an effective vibration suppression method, but control parameters for manipulator prototype is arduous to be adjusted to optimal solution. Trajectory planning optimization was first proposed by Kyung-Jo and Youn-Sik [18], they pointed out that residual vibration can not be minimized solely by minimizing position error of target point, and an optimized trajectory was design to minimize robot residual vibration. In contrast with above two methods, trajectory planning [18]–[25] is usually an offline optimization method, which takes elastic deformation or elastic potential energy as objective function, and joint trajectory as independent variables, to find a joint trajectory with minimum residual deformation or elastic potential energy, thereby achieve manipulator vibration suppression. In general, trajectory planning belongs to open–loop control, and has advantages of simple and direct, researchers presented

a mounts of flexible robot joint trajectories to minimum residual energy.

To speed up trajectory parameters optimization, researchers brought genetic algorithm into vibration suppression process [26]–[31]. Particle swarm optimization (PSO), which was first proposed by Kennedy [32], is a genetic algorithm with advantages of simple, small computation and less parameters to be adjusted [33]. Furthermore, researchers improved speed function by adding different parameter inertia weight into classical PSO in [34]–[36] and some improved PSO has attracted many researchers [37]–[41] to address a better way to suppress vibration. These researches focused on finding an optimal joint trajectories or optimized Cartesian trajectory in point to point trajectory planning. In joint trajectory planning optimization, some constraints are indispensable, such as joint trajectory interpolation point increments should be limited in small range in case of collision accident, manipulator endpoints interpolation point should be in a certain range. But classical PSO belongs to unconstrained optimization algorithm, it is not suitable for robot trajectory optimization under joint angle constraints. Consequently, a novel trajectory planning method based on modified PSO with penalty function named CP-PSO is proposed in this paper to find optimal joint trajectory with joint angle constraints.

Nevertheless, CP-PSO is still an offline optimization method by reason of much computation time. To uncertain task optimization, a sub-optimal trajectory that could be generated quickly is more acceptable. Accordingly, a rapid trajectory modified method is simultaneous proposed to optimize manipulator joint trajectory in real-time.

To sum up, two vibration suppression methods based on trajectory modified are proposed correspond to different operational scenarios. One is called CP-PSO, which is suitable for repetitive tasks in the case of trajectory optimization time is adequate, the other is rapid trajectory modified, appropriated for uncertain task which needs online vibration suppression and a sub-optimal trajectory is acceptable. The remainder of this paper is organized as follows. Section II details the problem formulation. In section III, two manipulator trajectory modified method are proposed. In section IV, the experiment results are reported, and section V concludes this paper.

II. PROBLEM FORMULATION

To analysis manipulator vibration from flexible joints, a simplified flexible joint model is established and then elastic potential of manipulator could be derived. With manipulator potential energy and kinetic energy, dynamic model of manipulator system based on Lagrangian method is formulated. Thus, relationship of joint output angle and joint rotor angle is presented.

A. SIMPLIFIED MODEL OF FLEXIBLE JOINT

A simplified model of flexible joint, which was first proposed by Spong [42], is used for analyzing the effect of joint flexibility on mechanical performance of robot joints. Whereas joint flexibility is mainly generated by harmonic reducer and torque sensor. Therefore, flexible joint model is simplified as a linear spring between joint motor rotor and the next link, which can be simply expressed as,

$$\begin{cases} M_i\ddot{q}_i = \tau_i \\ J_i\ddot{\theta}_i + \tau_i = \tau_{\mathrm{m}i} \\ \tau_i = K_i(\theta_i - q_i) \end{cases} \tag{1}$$

where q_i and θ_i respective denote joint output angle and joint motor rotor angle, M_i and J_i are joint output inertial matrix and joint motor inertial matrix respectively, τ_i and $\tau_{\mathrm{m}i}$ represent their torque separately, K_i refers joint stiffness.

Joint elastic potential of single joint in flexible joint model is given as,

$$V_{\mathrm{e}i} = \frac{1}{2}K_i(\theta_i - q_i)^2 \tag{2}$$

Hence, joint elastic potential of manipulator in flexible joint model can be expressed as,

$$V_{\mathrm{e}}(q,\theta) = \frac{1}{2}(\theta - q)^{\mathrm{T}}K(\theta - q) \tag{3}$$

B. DYNAMIC MODEL OF FLEXIBLE MANIPULATOR BASED ON LAGRANGIAN

Kinetic energy model of a flexible manipulator can be expressed as,

$$T(q,\dot{q},\dot{\theta}) = T_{\mathrm{l}}(q,\dot{q}) + T_{\mathrm{r}}(q,\dot{q},\dot{\theta}) \tag{4}$$

where $T_{\mathrm{l}}(q,\dot{q})$ is manipulator links' kinetic energy and $T_{\mathrm{r}}(q,\dot{q},\dot{\theta})$ is joint motor rotors' kinetic energy.

Potential energy could be defined as:

$$V(q,\theta) = V_{\mathrm{e}}(q,\theta) + V_{\mathrm{g}}(q) \tag{5}$$

where $V_{\mathrm{g}}(q)$ is gravitational potential energy.

Then, though calculation with equation (4) and (5), integrated model of flexible manipulator can be expressed as follows,

$$H(q)\begin{pmatrix}\ddot{q}\\ \ddot{\theta}\end{pmatrix} + \Gamma(q,\dot{q})\begin{pmatrix}\dot{q}\\ \dot{\theta}\end{pmatrix} + \begin{pmatrix} g(q) - K(\theta - q) \\ K(\theta - q)\end{pmatrix} = \begin{pmatrix}\tau_{\mathrm{ext}}\\ \tau_{\mathrm{m}}\end{pmatrix} \tag{6}$$

where $H(q)$ is inertia matrix, $g(q)$ represents gravity matrix, τ_{ext} refers external torque.

In our experiments, manipulator is a small rotor inertia robot. Thus, to simplify the manipulator integrated model, we assume that the translational energy of motor rotor is only determined by velocity of previous link, which is universal validity in small rotor inertia robots [43]. Then, simplified model of flexible joint robot can be expressed as,

$$\begin{cases} M(q)\ddot{q} + C(q,\dot{q})\dot{q} + g(q) = K(\theta - q) + \tau_{\mathrm{ext}} \\ J\ddot{\theta} + K(\theta - q) = \tau_{\mathrm{m}} \end{cases} \tag{7}$$

Some essential properties of the manipulator dynamics (7) are useful for deriving control algorithms, as follows,

Property 1: The inertial matrix $M(q)$ is uniformly positive definite and symmetric. $mC(q,\dot{q})$ can be reformulated as $(I \otimes \dot{q}^{\mathrm{T}})C_v(q)\dot{q}$.

Property 2: $(\dot{M}(q) - 2C(q,\dot{q}))$ is skew-symmetric so that $v^{\mathrm{T}}(\dot{M}(q) - 2C(q,\dot{q}))v = 0$ for all $n \times 1$ vector v.

Property 3: The manipulator dynamics (7) is linear in a set of physical parameters.

$$M(q)\ddot{q} + C(q,\dot{q})\dot{q} + g(q) = Y(q,\dot{q},\ddot{q})\theta_d \tag{8}$$

where the dynamic regression matrix $Y(q,\dot{q},\ddot{q})$ is bounded for bounded argument signals.

C. JOINT OUTPUT ANGLE BASED ON FOUR-ORDER IMPLICIT RUNGE-KUTTA

Due to joint flexibility, a joint angle error exists between joint output and joint motor during joint movement, which means joint output can not track motion of joint motor in time. Naturally, joint motor angle θ could be obtained from the desired trajectory, and joint output angle q could be calculated with equation (7), that is, the state equation can be expressed as,

$$\dot{x} = f(x,\theta) \tag{9}$$

where $\dot{x} = (\dot{x}_1\ \dot{x}_2)^{\mathrm{T}}$,

$$f = \left[x_2\ M^{-1}(x_1)(K(\theta - x_1) - C(x_1,x_2)x_2 - g(x_1))\right]^{\mathrm{T}}.$$

Equation (9) is rigid differential equation because stiffness coefficient of joint is large constant, which iterative step size must be limited in a small range to ensure stability of algorithm. Namely, computation time is too long and result is inaccurate owing to iterative steps is too many for a long interval.

Generally, implicit solution is suitable for solving rigid differential equation since algorithm stability of implicit solution is independent of iterative step size. In this paper, a two-stage four-order implicit Runge-Kutta method is used to solve the rigid differential equation, which iterative formula is given as,

$$\begin{cases} x_{n+1} = x_n + \dfrac{h}{2}(k_1 + k_2) \\ k_1 = f\left(\theta, x_n + \dfrac{h}{2}\left(k_1 + \left(1 + \dfrac{2\sqrt{3}}{3}\right)k_2\right)\right) \\ k_2 = f\left(\theta, x_n + \dfrac{h}{2}\left(\left(1 - \dfrac{2\sqrt{3}}{3}\right)k_1 + k_2\right)\right) \end{cases} \tag{10}$$

D. RELATIONSHIP BETWEEN RESIDUAL DEFORMATION AND JOINT TRAJECTORY

Generally, joint angle deformation δ_θ is obtained from joint output angle and joint motor angle, which can be defined as,

$$\delta_\theta = \theta - q \tag{11}$$

Elastic potential energy from joint angle deformation can be expressed as,

$$V_d = \frac{1}{2}\delta_\theta^{\mathrm{T}} K \delta_\theta \tag{12}$$

The relationship between elastic potential energy and joint angle is shown in formula (11) and (12). Thus, residual elastic potential energy of manipulator can be obtained after robot reaching target position, which can be used as objective function in trajectory optimization.

III. METHOD

A. OFF-LINE TRAJECTORY OPTIMIZATION BASED ON PSO

In this section, in order to find an optimized trajectory with minimum residual elastic potential energy, an offline joint trajectory optimization method based on Particle Swarm Optimization (PSO) is adopted.

PSO is an evolutionary algorithm and an optimization tool based on iteration. But unlike genetic algorithm, there is no crossover or mutation in PSO. However, classical PSO has typical drawbacks in trajectory planning. For instant, there are many parameters (such as learning factor and inertia weight) in PSO, each particle's flying speed and weight of inheriting between itself and the group need to be adjusted for different particles and objective function. In addition, PSO belongs to optimization method without variable constrains. However, if joint interpolation points were not constrained during joint trajectory optimization, unsafe joint trajectory may be generated, which may lead to dangerous situation such as collision accident.

In summary, a novel PSO is proposed to optimize joint trajectory, penalty function will be included in the new PSO to deal with joint interpolation increments constraint. Then a new objective function is generated, joint trajectory optimization with joint angle limited is implemented.

1) CLASSICAL PSO

In classical PSO, each particle has one corresponding objective function value and flying speed. Search space is a d dimensional space, which is quantity of interpolation point increments, and a group of increments refers to one new trajectory. Assuming that there are n particles in a particle swarm, then, position and velocity of ith particle can be expressed as $X^i = (x_{i,1}, x_{i,2} \cdots x_{i,d})$ and $V^i = (v_{i,1}, v_{i,2} \cdots v_{i,d})$ respectively. In each step, particle updates itself by tracking two optimal solutions, One optimal solution found by itself is named p_{best}, which is expressed as $P^i = (p_{i,1}, p_{i,2} \cdots p_{i,d})$, the other one optimal solution found in whole group is named g_{best}, which is expressed as $P^g = (p_{g,1}, p_{g,2} \cdots p_{g,d})$. Particle updates itself with these two optimal values and the update formula is,

$$\begin{cases} v_{i,j}(k+1) = wv_{i,j}(k) + c_1 r_1[p_{i,j} - x_{i,j}(k)] \\ \qquad\qquad + c_2 r_2[p_{g,j} - x_{i,j}(k)] \\ x_{i,j}(k+1) = x_{i,j}(k) + v_{i,j}(k+1) \end{cases} \tag{13}$$

where w is inertial factor, c_1 refers self-learning factor, c_2 represents group-best-learning factor, r_1 and r_2 are two independent uniform random numbers with values from 0 to 1.

2) PSO WITH COMPRESSION FACTOR

Different learning factor c_1 and c_2 will generate distinct particle flying trajectory. In other words, particle will wander in the local area with a larger self-learning factor, simultaneity, a larger group-best-learning factor will lead particle converging in a local minimum prematurely. To effectively balance particle's flying speed in global search and local search, Clerc [35] proposed a PSO algorithm with compression factor. The speed function is replaced with,

$$v_{i,j}(k+1) = \varphi\{v_{i,j}(k) + c_1 r_1[p_{i,j} - x_{i,j}(k)] + c_2 r_2[p_{g,j} - x_{i,j}(k)]\} \quad (14)$$

where φ is a constriction factor, it is defined as,

$$\varphi = 2/\left|2 - C - \sqrt{C^2 - 4C}\right|, \quad C = c_1 + c_2,\ C > 4.$$

Typically, c_1 and c_2 are both set to 2.05 [36], [41].

3) COMPRESSION FACTOR PSO WITH PENALTY FUNCTION (CP-PSO)

PSO with compression factor is incapable of trajectory planning with joint angle interpolations limited. In this paper, we introduce penalty function to enlarge value of objective function, thereby the new objective function could ensures particles (which are response to different groups of interpolation points' increment) that not satisfied with constraint are eliminated. For this, we build a function $g_j(x)$ to represent interpolation limited, $g_j(x) = -1$ means constraint is not satisfied, and if constraint is satisfied, $g_j(x) = 1$. Then we set penalty factor K_{penalty} outweigh original objective function value which can be obtain in the first iteration, it will ensure value of new objective function is large enough to eliminate particles hat not satisfied with constraint. The combination of joint angle interpolations limited and objective function with compression factor is expressed as,

$$F(x) = f(x) + K_{\text{penalty}} \sum_{j=1}^{m} \left[\min(0, g_j(x))\right]^2 \quad (15)$$

where $F(x)$ is new objective function of CP-PSO. $f(x)$ refers objective function of PSO with compression factor, which is sum of residual elastic potential from all joints. K_{penalty} is penalty factor. $g_j(x)$ represents interpolation limited, $g_j(x) = -1$ means constraint is not satisfied and $g_j(x) = 1$ if constraint is satisfied.

The new objective function is used as CP-PSO objective function to search joint angle interpolation increments. When constraint is not satisfied, a large penalty value is generated and particles will be eliminated. In contrast, particles satisfy the constraint will be saved and used in next iteration.

B. VIBRATION SUPPRESSION BASED ON RAPID TRAJECTORY MODIFIED

CP-PSO is an off-line optimization method since it cost large amounts of computation time, which is suitable for joint trajectory optimization in fixed trajectory task. But to uncertain operational tasks, robot requires a rapid trajectory modified ability. Compared with optimal joint trajectory from CP-PSO, a sub-optimal solution that can be generated in a short time is a better choice.

Vibration suppression is a cumulative process rather than a sudden process. As a result, a vibration prediction criteria can be established to vibration trend prediction. Simultaneously, a three-section DKA modified trajectory is proposed, initial joint trajectory is replaced with modified trajectory to eliminate vibration tendency. Finally, combination of vibration prediction criteria and modified trajectory can be executed in robot central controller and satisfies real-time trajectory modified requirement.

1) VIBRATION PREDICTION CRITERION BASED ON TORQUE SENSOR

Joint torque sensor could real-time collect joint torque information, which intuitively reflects joint torque amplitude during robot vibration. For example, large amplitude vibration corresponds to large joint torque in most cases. Additionally, torque signal of flexible robot is constantly fluctuating during joint motion. Moment amplitude of torque fluctuation exceeds a threshold value indicates that robot has vibrated. By observing and analyzing the torque signal during robot motion, vibration can be predicted before robot vibration is visible to naked eyes, then modified trajectory will be switched on to avoid vibration before amplitude of torque fluctuations constantly increases.

Due to tracking accuracy and other uncertainties, joint torque error exists between measured value and theoretical value of joint torque, which reflects joint deformation, and corresponds to vibration amplitude of joint. It is possible to predict joint vibration will occur before joint deformation constantly increases. Joint torque error can be defined as,

$$\tau_{\text{error}} = \tau_{\text{theo}} - \tau_{\text{measu}} \quad (16)$$

where τ_{error} is joint torque error; τ_{theo} refers theoretical value of the joint torque based on dynamic model and desired trajectory; τ_{measu} represents joint torque from joint torque sensors in actual trajectory.

As mentioned above, most robot vibration is process of torque fluctuations amplitude increasing rather than happening in a sudden. A criterion of vibration prediction is established based on two threshold value - joint torque error threshold and maintenance time. The criterion consists of two conditions as shown below,

Condition 1: The absolute value of joint torque error τ_{error} exceeds threshold of joint torque error τ_{elimit}. In general, τ_{elimit} is set as half of torque error when manipulator has obvious vibration;

Condition 2: Condition 1 happens k_{limit} times with absolute value of τ_{error} constantly increasing and time interval between two adjacent condition 1 is less than Δt_{limit}. This condition is used to avoid joint torque error by accident, k_{limit} should more than once and Δt_{limit} should be enough to generate joint torque error points.

The algorithm of the proposed method is briefly summarized in Algorithm 1.

Algorithm 1 Vibration Prediction Criterion

Initialize τ_{elimit}, Δt_{limit}, k_{limit} with initial joint torque error
for $k = 1$ to k_{limit} do
  $\tau_{\text{error}} \leftarrow \text{torque\_error}(\tau_{\text{theo}}, \tau_{\text{measu}})$
  if $\text{abs}(\tau_{\text{error}}) > \tau_{\text{elimit}}$ do
    $t(k) \leftarrow t_{\text{now}}$; $\tau(k) \leftarrow \tau_e$
  end if
  if not $k > 1$ then
    $k = k + 1$
    continue
  end if
  if $\tau(k) > \tau(k-1), t(k) - t(k-1) < \Delta t_{\text{limit}}$ then
    $k = k + 1$
    continue
  else if
    break;
  end if
  if $k = k_{\text{limit}}$ then
    return true
    end if
end for
return false

2) THREE-SECTION DKA MODIFIED TRAJECTORY

Vibration of robot is more likely to happen in highly velocity motion than in low velocity motion. Therefore, a three-section DKA modified trajectory is proposed, increasing vibration amplitude is eliminated by decelerating joint velocity. Three-section DKA modified trajectory consists of smooth decelerating process, low velocity keeping process and accelerating process.

In the proposed modified trajectory, smooth decelerating process is used to lower joint velocity to reduce joint torque error, and robot vibration tendency is eliminated while joint velocity decreases. Low velocity keeping process and accelerating process are used to guarantee running time. In addition, joint velocity increases gradually in accelerating process, vibration prediction criterion is restarted to monitor joint torque, three-section DKA trajectory modified method will be executed when vibration is predicted to happen. The corresponding modified trajectory function is introduced as,

a: SMOOTH DECELERATING PROCESS

In order to achieve velocity smooth decelerating and maintain acceleration continuity between smooth decelerating process and low velocity keeping process, smooth decelerating process has two requirements as follows,

First, maintain joint angle θ_{sd0}, velocity $\dot{\theta}_{\text{sd0}}$, and acceleration $\ddot{\theta}_{\text{sd0}}$ at starting point of smooth decelerating process as same as initial trajectory when vibration is predicted to happen with vibration prediction criterion, the starting time of smooth decelerating process is marked as t_{sd0}.

Secondly, joint acceleration is 0 and joint velocity is reduced to a predetermined velocity $\dot{\theta}_{\text{sdd}}$ at the end of smooth decelerating process,

$$\dot{\theta}_{\text{sdd}} = K_{\text{v}} \dot{\theta}_{\text{sd0}} \tag{17}$$

where, $K_{\text{v}} (K_{\text{v}} < 1)$ refers decelerating velocity factor.

The duration of smooth decelerating process $(t_{\text{lvk0}} - t_{\text{sd0}})$ is defined as,

$$t_{\text{lvk0}} - t_{\text{sd0}} = K_{\text{t1}} T_{\text{sd}} = K_{\text{t1}} (T - t_{\text{sd0}}) \tag{18}$$

where, K_{t1} $(K_{\text{t1}} < 1)$ is decelerating velocity time factor, T_{sd} $(T_{\text{sd}} = T - t_{\text{sd0}})$ represent remaining time. t_{lvk0} refers the end time of smooth decelerating process and also the starting time of low velocity keeping process. T represents desired trajectory running time.

To generate modified trajectory in smooth decelerating process, modified three-order spline is utilized, which consists of three sections. Specifically, the first and third section function is five-order spline to maintain acceleration continuity, and the middle section function is classical three-order spline. In addition, joint interpolation points are generated with initial joint trajectory. That is to say, joint velocity can be reduced to predetermined velocity and joint trajectory goes through joint interpolation points generated with initial joint trajectory.

Modified three-order spline function is constructed as,

$$\begin{cases} \theta_{\text{sd1}}(t) = \lambda_{13}(t - t_{\text{sd0}})^3 + \lambda_{12}(t - t_{\text{sd0}})^2 + \lambda_{11}(t - t_{\text{sd0}}) \\ \qquad + \lambda_{10} + \lambda_{f1}(t - t_{\text{sd2}})^3 (t - t_{\text{sd0}})^2 \\ \theta_{\text{sd2}}(t) = \lambda_{23}(t - t_{\text{sd2}})^3 + \lambda_{22}(t - t_{\text{sd2}})^2 \\ \qquad + \lambda_{21}(t - t_{\text{sd2}}) + \lambda_{20} \\ \theta_{\text{sd3}}(t) = \lambda_{33}(t - t_{\text{sd3}})^3 + \lambda_{32}(t - t_{\text{sd3}})^2 \\ \qquad + \lambda_{31}(t - t_{\text{sd3}}) + \lambda_{30} \\ + \lambda_{f3}(t - t_{\text{sd3}})^3 (t - t_{\text{lvk0}})^2 \end{cases} \tag{19}$$

where λ_{ij} represents coefficient of three-order spline, i refers corresponding section of spline, j is corresponding order of spline function; λ_{fi} represents coefficient of five-order spline; $t_{\text{sd}i}$ refers starting time of corresponding section of spline.

All coefficients can be get according to given conditions,

$$\begin{cases} \theta_{\text{sd1}}(t_{\text{sd0}}) = \theta_{\text{sd0}}, \dot{\theta}_{\text{sd1}}(t_{\text{sd0}}) = \dot{\theta}_{\text{sd0}}, \ddot{\theta}_{\text{sd1}}(t_{\text{sd0}}) = \ddot{\theta}_{\text{sd0}} \\ \theta_{\text{sd1}}(t_{\text{sd2}}) = \theta_{\text{sd2}}(t_{\text{sd2}}) = \theta_{\text{sd2}} \\ \dot{\theta}_{\text{sd1}}(t_{\text{sd2}}) = \dot{\theta}_{\text{sd2}}(t_{\text{sd2}}), \ddot{\theta}_{\text{sd1}}(t_{\text{sd2}}) = \ddot{\theta}_{\text{sd2}}(t_{\text{sd2}}) \\ \theta_{\text{sd2}}(t_{\text{sd3}}) = \theta_{\text{sd3}}(t_{\text{sd3}}) = \theta_{\text{sd3}} \\ \dot{\theta}_{\text{sd2}}(t_{\text{sd3}}) = \dot{\theta}_{\text{sd3}}(t_{\text{sd3}}), \ddot{\theta}_{\text{sd2}}(t_{\text{sd3}}) = \ddot{\theta}_{\text{sd3}}(t_{\text{sd3}}) \\ \theta_{\text{sd3}}(t_{\text{lvk0}}) = \theta_{\text{lvk0}}, \dot{\theta}_{\text{sd3}}(t_{\text{lvk0}}) = \dot{\theta}_{\text{sdd}}, \ddot{\theta}_{\text{sd3}}(t_{\text{lvk0}}) = 0 \end{cases} \tag{20}$$

where $\theta_{\text{sd}i}$ is joint interpolation points from initial trajectory.

b: LOW VELOCITY KEEPING PROCESS

In low velocity keeping process, joint runs at a uniform velocity of $\dot{\theta}_{\text{sdd}}$, the duration of low velocity keeping process $(t_{a0} - t_{\text{lvk0}})$ is defined as,

$$t_{a0} - t_{\text{lvk0}} = K_{\text{t2}} T_{\text{sd}} \tag{21}$$

where K_{t2} ($K_{t2} < 1$) refers low velocity time factor. t_{a0} refers the end time of low velocity keeping process and also the starting time of accelerating process.

Trajectory in low velocity keeping process is given as,

$$\theta_{lvk}(t) = \dot{\theta}_{sdd}(t - t_{lvk0}) + \theta_{sd3}(t_{lvk0}) \tag{22}$$

c: ACCELERATING PROCESS

Compared with the foresaid two sections, accelerating process is a "trajectory catching up" section to maintain modified trajectory running time equal with desired trajectory running time. There are six constraints in accelerating process:

Joint angle, velocity and acceleration at the starting of accelerating process remain same with the end of low velocity keeping process. Joint angle of the end of accelerating process reaches desired target angle, joint velocity and acceleration reduced to 0 gradually when joint is approaching to target angle. Thus trajectory function is replaced with five-order spline which is defined by,

$$\begin{aligned}\theta_a(t) = {} & \lambda_{a5}(t - t_{a0})^5 + \lambda_{a4}(t - t_{a0})^4 + \lambda_{a3}(t - t_{a0})^3 \\ & + \lambda_{a2}(t - t_{a0})^2 + \lambda_{a1}(t - t_{a0}) + \lambda_{a0}\end{aligned} \tag{23}$$

where λ_{ai} is coefficient of five-order spline.

All coefficients could be calculated according to given conditions,

$$\begin{cases} \theta_a(t_{a0}) = \theta_{lvk}(t_{a0}), \dot{\theta}_a(t_{a0}) = \dot{\theta}_{lvk}(t_{a0}), \\ \ddot{\theta}_a(t_{a0}) = \ddot{\theta}_{lvk}(t_{a0}) \\ \theta_a(T) = \theta_{lvk0}, \dot{\theta}_a(T) = 0, \ddot{\theta}_a(T) = 0 \end{cases} \tag{24}$$

IV. EXPERIMENTS AND DISCUSSIONS

A. OFF-LINE VIBRATION SUPPRESSION WITH JOINT INTERPOLATION POINT INCREMENTS LIMITED

In this section, joint trajectory is optimized with CP-PSO to suppress manipulator residual vibration. By analyzing the configuration of manipulator, joint vibration, which is far from end-effector, has more influence on extremity of manipulator. Therefore, first four joint trajectories are optimized with CP-PSO to simplify dynamic model of manipulator and improve the efficiency of CP-PSO.

Joint trajectory between initial joint angles A $= [-48.2°, -20.4°, 42.8°, 66.9°]$ and target joint angles B $= [-40.7°, -33.1°, 70.1°, 62.5°]$ is chosen as an example. The trajectory running time sets to 20s.

To optimize joint trajectory of those four joints, interpolation points $\hat{\theta}_i^k$ are assumed as key points to avoid collision during joint motion. In this experiment, initial joint interpolation points $\hat{\theta}_i^k$ are generated with three-order spline function and constant time interval. Namely, manipulator should move with optimal joint trajectory, which joint interpolation points' increment is limited in a specified range to avoid collision.

To generate trajectory between joint interpolation points, three-order spline function is adopted, which means joint angle, velocity and acceleration are continuous at each joint interpolation point. Then, five-order spline function is employ to modify the first and the last segments to keep starting acceleration and ending acceleration of whole joint trajectory is 0. Take joint 1 for example, joint interpolation points $\hat{\theta}_i^k$ and initial joint trajectory is shown in figure 1.

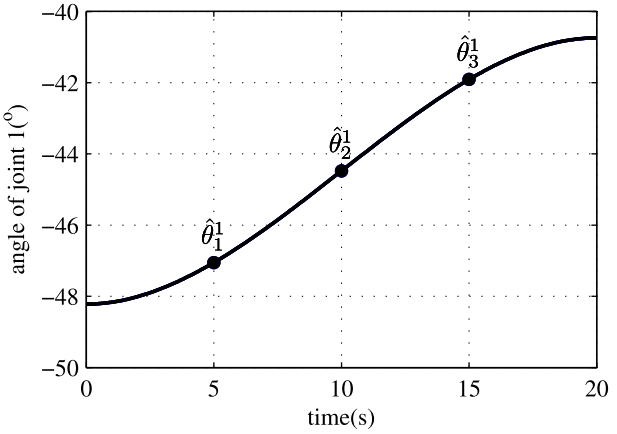

FIGURE 1. Initial joint trajectory interpolation points of joint 1.

CP-PSO is used to search the best joint trajectory interpolation points' increment $\Delta\theta_i^k$. Assume that manipulator will not collide when interpolation point increments is less than 2°, which means penalty function is,

$$g_j(x) = sign(2 - abs(\Delta\theta_j^k)) \tag{25}$$

In consequence, fitness function of CP-PSO is given as,

$$F_E(x) = \frac{1}{2}\delta_R^T(\theta)K\delta_R(\theta) + K_{penalty}\sum_{j=1}^{m}(\min(0, g_j(x)))^2 \tag{26}$$

where $\delta_R(\theta)$ is joint residual elastic deformation, $\theta(t)$ refers joint trajectory, K represents stiffness matrix of manipulator.

When learning factor $c_1 = c_2 = 2.05$ [41], compression factor $\varphi = 0.729$, CP-PSO iterate time $m = 200$, manipulator residual elastic potential energy under initial joint trajectory is $V_d = 0.155$J, to limit interpolation point increments is less than 2° strictly, penalty factor $K_{penalty}$ must far outweigh V_d, thus, $K_{penalty} = 100$ in this simulation. Five-order spline trajectory and cycloid trajectory between joint angles A and B are chosen as control group. Manipulator residual elastic potential energy under five-order trajectory and cycloid trajectory are $V_{d,f} = 0.156$J and $V_{d,c} = 0.186$J respectively.

Joint angle, velocity and acceleration of initial trajectory, five-order spline trajectory, cycloid trajectory and optimized trajectory are demonstrated in figure 2, figure 3 and figure 4 respectively. In these figures, black line is initial information, black dot line is five-order spline information, black dot-dash line is cycloid trajectory information, and the red dashed line is optimized information. Initial joint trajectory, five-order spline trajectory, cycloid trajectory almost overlap. Which means angle, velocity and acceleration are almost the same.

From figure 2, increments $\Delta\theta_i^k$ in each joint trajectory interpolation point is tightly limited in 2°. Figure 3 shows optimized joint velocities are all under 3°/s, which is less than

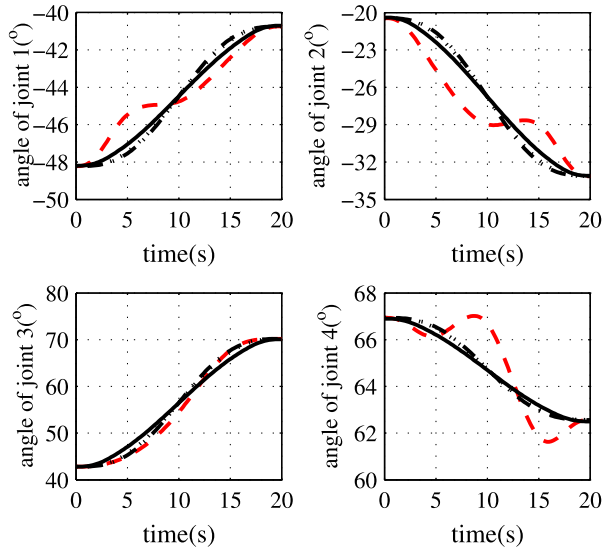

FIGURE 2. Joint angle of initial trajectory, five-order spline trajectory, cycloid trajectory and optimized joint trajectory.

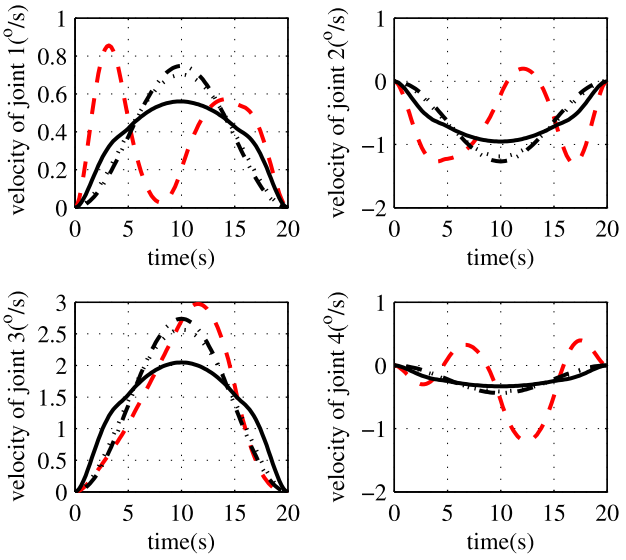

FIGURE 3. Joint velocity of initial trajectory, five-order spline trajectory, cycloid trajectory and optimized joint trajectory.

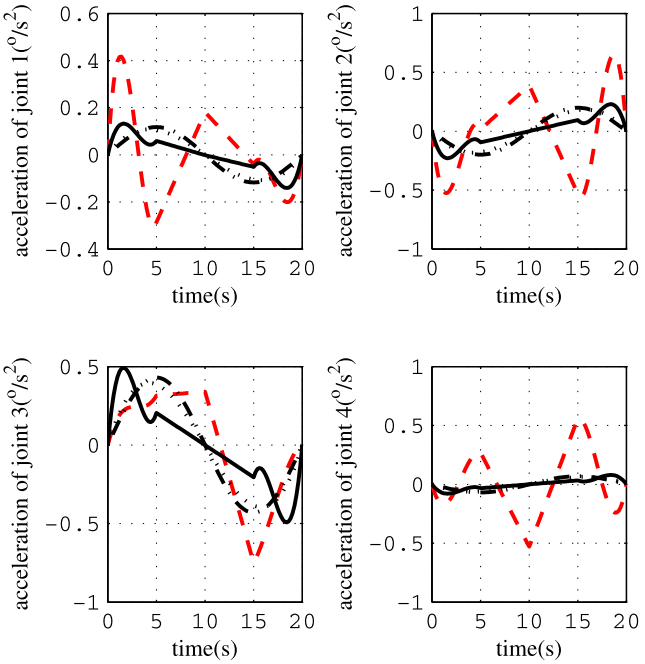

FIGURE 4. Joint acceleration of initial trajectory, five-order spline trajectory, cycloid trajectory and optimized joint trajectory.

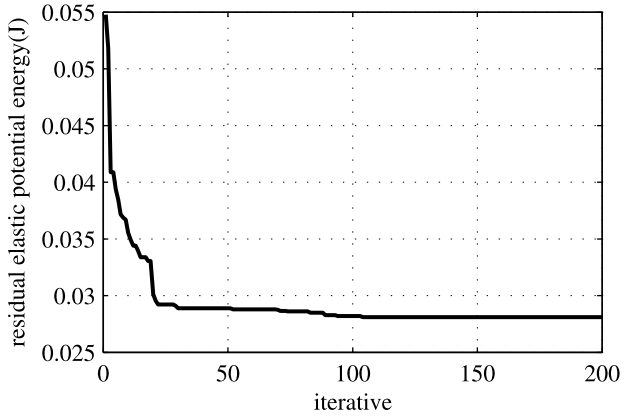

FIGURE 5. Variation of joint residual potential energy.

real manipulator joint nominal velocity. Figure 4 indicates optimized joint accelerations are under joint maximum acceleration. In other words, optimized joint trajectories satisfy trajectory interpolation point increments $\Delta\theta_i^k \leq 2°$ and can be executed in manipulator prototype.

Variation of joint residual elastic deformation with iteration manifests in figure 5. Figure 5 demonstrates manipulator residual potential energy is significantly reduced to 0.0281J. Optimized trajectory is superior to initial trajectory, five-order trajectory and cycloid trajectory with minimum residual potential energy.

To validate optimized joint trajectory shown in figure 2, the optimized joint trajectory is used to drive manipulator prototype. Then residual vibration with optimized joint trajectory is compared with spline joint trajectory and linear trajectory in Cartesian space.

By analyzing manipulator configuration, we found that manipulator vibration is mainly caused by shoulder joint in most cases. Therefore, torque information of shoulder joint under three trajectories are given as indication in figure 6, figure 7 and figure 8, which is corresponding to optimized joint trajectory and spline joint trajectory and line trajectory in Cartesian space.

Compared with figure 7 and 8, figure 6 demonstrates that optimized joint trajectory is obviously improved in amplitude and duration of residual vibration than spline joint trajectory. Residual vibration with linear trajectory in Cartesian space is most obvious and lasts for the longest time.

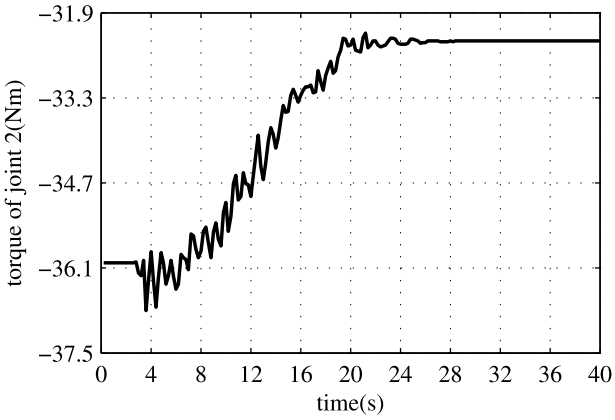

FIGURE 6. Shoulder joint torque of optimized joint trajectory.

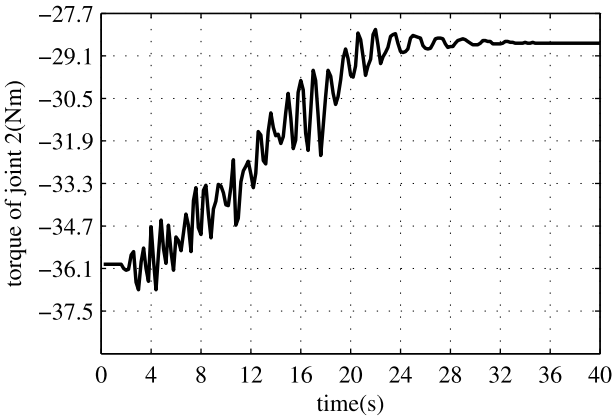

FIGURE 7. Shoulder joint torque of spline joint trajectory.

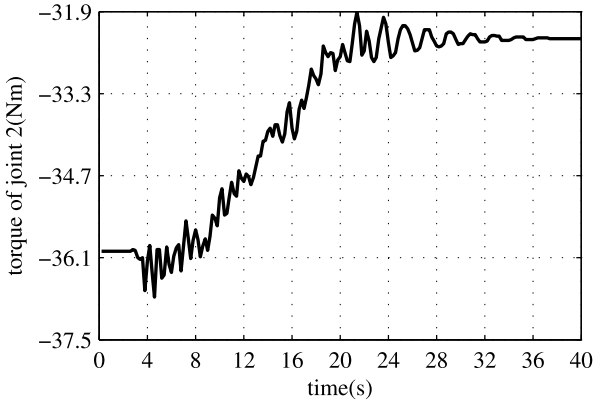

FIGURE 8. Shoulder joint torque of line trajectory in Cartesian space.

The result shows CP-PSO is effective in search of optimized joint trajectory that corresponding to minimum residual elastic potential energy, which means residual vibration is suppressed evidently. In addition, variation of shoulder joint torque in optimized joint trajectory is minimum, which means vibration during motion decreases. It can be explained that the optimized joint trajectory is the optimal joint trajectory for vibration suppression.

B. OFF-LINE VIBRATION SUPPRESSION WITH CARTESIAN POSITION ERROR LIMITED

In second experiment, a circular Cartesian trajectory (center at [0.7 0] and radius is 0.2m) of manipulator endpoint is chosen to generated initial joint trajectory. Initial joint trajectories of circular Cartesian manipulator endpoint trajectory is generated with 12 control positions, those control positions are uniformly distributed on manipulator endpoint circular Cartesian trajectory. The corresponding joint angles are set as interpolation points of joint trajectories, trajectories between interpolation points are generated in same way as first experiment. Initial manipulator endpoint Cartesian trajectory is shown in figure 9.

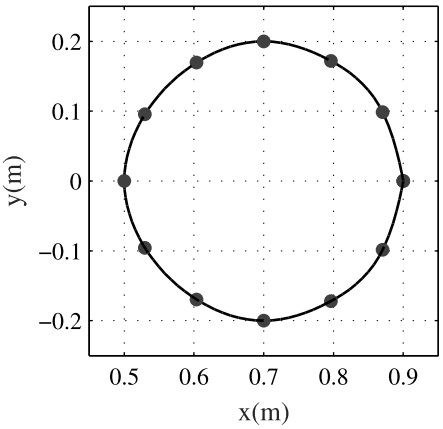

FIGURE 9. Manipulator endpoint Cartesian trajectory.

As same as previous experiment, learning factor $c_1 = c_2 = 2.05$, compression factor $\varphi = 0.729$, CP-PSO iterate time $m = 200$, manipulator residual elastic potential energy under initial joint trajectory is $V_d = 8.725$J, penalty factor K_{penalty} must far outweigh V_d, thus, penalty factor $K_{\text{penalty}} = 100$ in this simulation.

Four optimizations with different penalty function are carried out. The corresponding penalty function is listed below,

Case 1 Joint trajectories is optimal without limit, penalty function $g_{1,j}(x) = 0$.

Case 2 Joint trajectories is optimal with interpolation point increments is less than 2 degree, penalty function $g_{2,j}(x) = sign(2 - abs(\Delta\theta_j^k))$.

Case 3 Joint trajectories is optimal with manipulator endpoint error is less than 10mm, penalty function $g_{3,j}(x) = sign(10 - abs(\Delta P_{\text{eer},j}))$.

Case 4 Joint trajectories is optimal with no limit, penalty function $g_{4,j}(x) = g_{2,j}(x) + g_{3,j}(x)$.

Optimized manipulator endpoint trajectory demonstrate in figure 10, figure 11, figure 12 and figure 13 respectively. In those figures, black line refers initial manipulator endpoint Cartesian trajectory, the red dashed line represents optimized manipulator endpoint Cartesian trajectory. Green dot at each interpolation point is a 10mm circular disk, optimized control position should be in the disk if it satisfies manipulator endpoint error is less than 10mm.

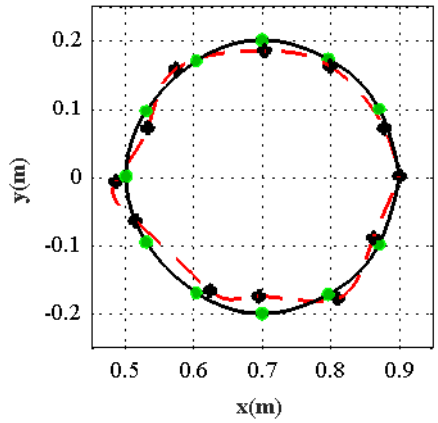

FIGURE 10. Manipulator endpoint trajectory without limit.

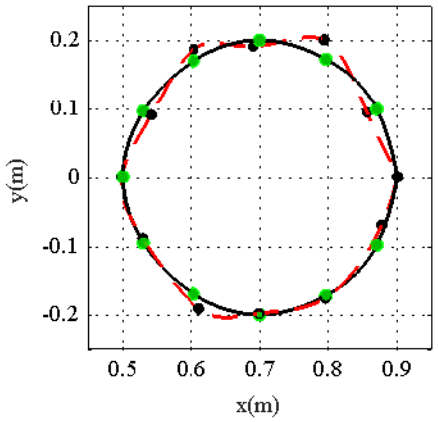

FIGURE 11. Manipulator endpoint trajectory with joint interpolation point increments is less than 2°.

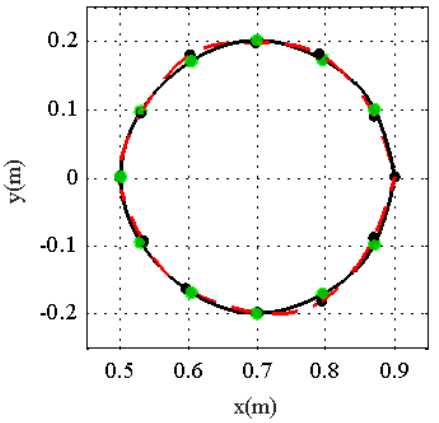

FIGURE 12. Manipulator endpoint trajectory with manipulator endpoint error is less than 10mm.

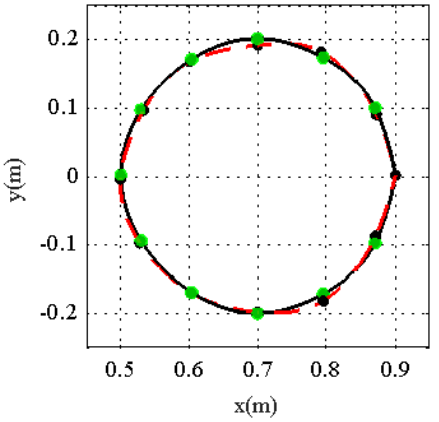

FIGURE 13. Manipulator endpoint trajectory with joint interpolation point increments less than 2 degree and endpoint error less than 10mm.

Figure 10 and 11 indicate joint trajectory optimization without limit or just under interpolation point increments restrict some position errors at optimized manipulator endpoint trajectory interpolation points are much too large, it means manipulator endpoint trajectory changes dramatically.

Figure 12 and 13 demonstrate that optimized joint trajectories under **Case 3** or **Case 4** could achieve vibration suppression and maintain manipulator endpoint Cartesian trajectory in a specified range at the same time. In other words, joint trajectory could be optimized with different constraints.

C. RAPID VIBRATION SUPPRESSION EXPERIMENT

One joint motion experiment is used to confirm vibration suppression with rapid modified trajectory. Set joint angle moving from 0 to 40° and trajectory running time $T = 20$s. Then the initial joint trajectory is shown in figure 14. Joint torque during motion demonstrates in figure 15, whereas joint torque error manifests in figure 16.

As shown in figure 16, joint torque error increases along with joint motion. When torque error exceeds 2Nm during initial manipulator running, manipulator obviously vibrate

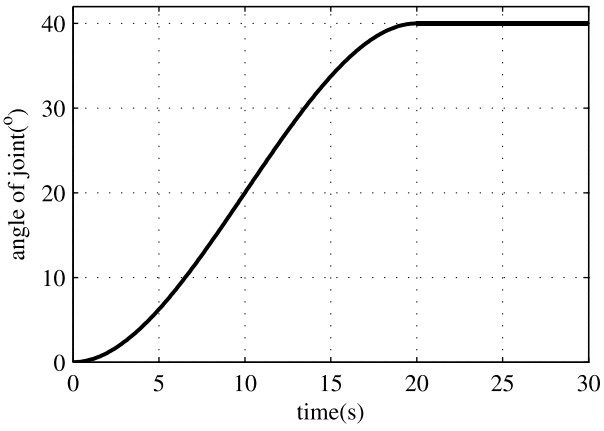

FIGURE 14. Initial joint trajectory.

by naked eyes. Therefore, set threshold of joint torque error τ_{elimit} to half of the torque error when manipulator has noticeable vibration, that is, $\tau_{\text{elimit}} = 1$Nm. Set threshold of time interval $\Delta t_{\text{limit}} = 1$s, $k_{\text{limit}} = 5$. Figure 16 illustrates that vibration is predicted to happen in 6.1s due to joint torque

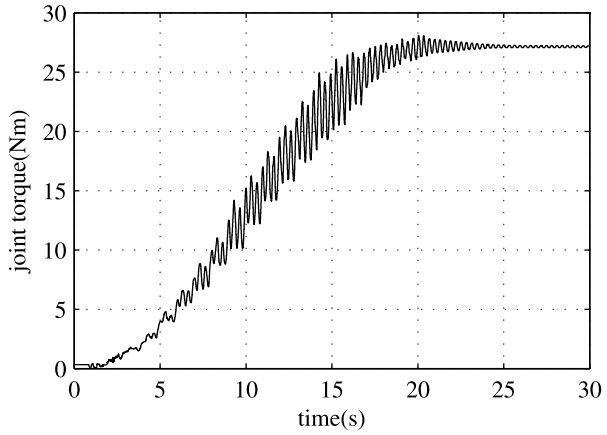

FIGURE 15. Joint torque of initial joint trajectory.

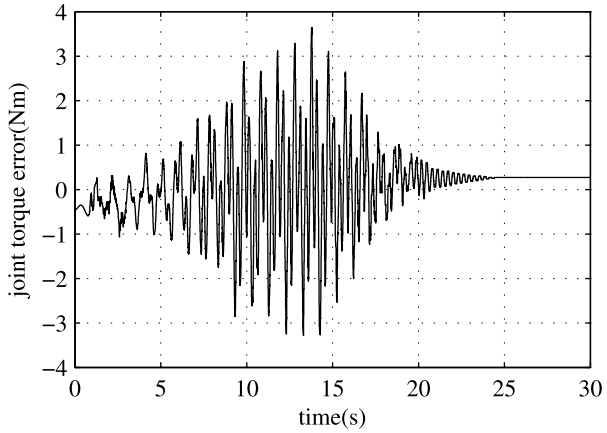

FIGURE 16. Joint torque error of initial joint trajectory.

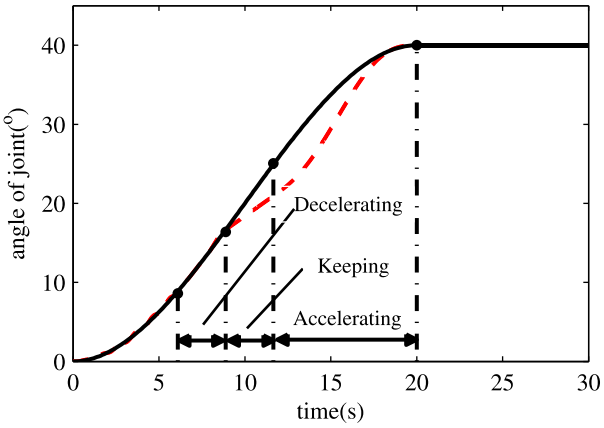

FIGURE 17. Initial and modified joint trajectory.

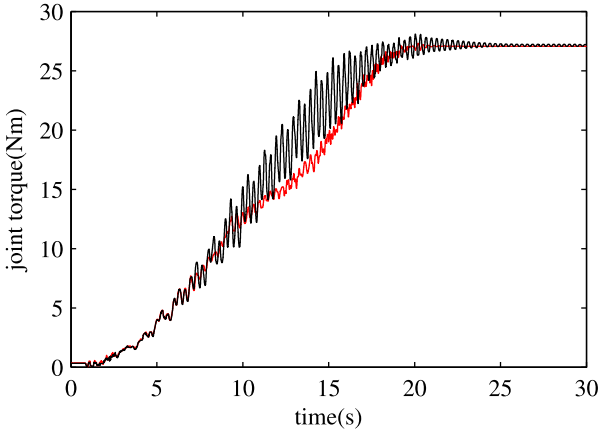

FIGURE 18. Joint torque of initial and modified joint trajectory.

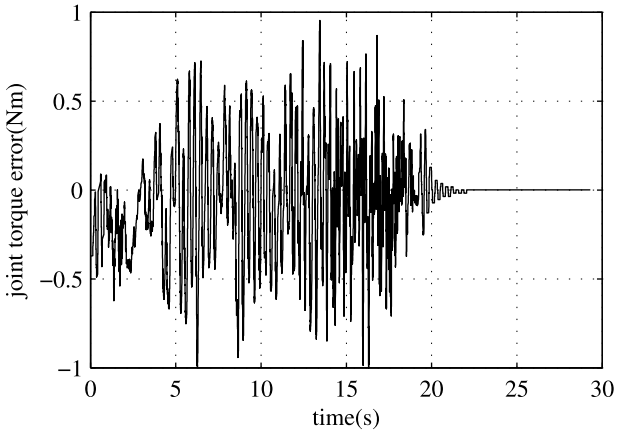

FIGURE 19. Joint torque error of modified joint trajectory.

error repeatedly exceed 1Nm in 1s, then three-section DKA modified trajectory should be switched on.

In three-section DKA modified trajectory, set decelerating velocity factor $K_v = 0.6$, it is a tradeoff of joint velocity reduces obviously and easy to catch up trajectory on time. Decelerating time factor during smooth decelerating process is set as $K_{t1} = 0.2$, which is enough to decrease joint velocity. Low velocity time factor during low velocity keeping process sets as $K_{t2} = 0.2$, it is a quite long time to avoid vibration still happen in low velocity keeping process.

With formula $19 \sim 26$, initial joint trajectory and modified trajectory is shown in figure 17, black line refers initial joint trajectory, and the red dash line is modified trajectory. The corresponding joint torque information demonstrates in figure 18, black line represents joint torque of initial trajectory, the red line is joint torque of modified trajectory. Joint torque error of modified trajectory details in figure 19.

Figure 18 and 19 demonstrate joint torque fluctuation of manipulator in modified joint trajectory is significantly smaller than initial joint trajectory, which means modified joint trajectory reduces vibration during motion and restrains potential vibration. In summary, the proposed three-section DKA trajectory modified method could suppress vibration effectively.

In summary, experiments are carried out to validate the proposed CP-PSO in joint trajectory optimization offline and online trajectory modified to decrease manipulator vibration. Experiment A gives a joint trajectory optimization to minimize residual potential energy when joint interpolation

points' increment are limited in 2°, and optimized joint trajectory is executed in manipulator prototype, joint torque fluctuation decreases significantly. Trajectory optimizations under four different constraints are contrasted in experiment B, experimental results illustrate that trajectory can be optimized with different constraints by proper penalty functions. Experiment C indicates that joint vibration can be accurate predicted with vibration prediction criterion and effectively suppressed by proposed DKA trajectory. Joint trajectory modified with vibration prediction criterion and DKA trajectory could suppress vibration online.

V. CONCLUSIONS

In order to suppress robot vibration with specified constraints, a novel PSO named CP-PSO is proposed to optimize joint trajectory. In CP-PSO, penalty function is introduced to eliminate particles which not satisfied joint angle constraints, therefore, part shortage of classical PSO is offset. But CP-PSO still consumes large amount of computation time, which is just suitable for fixed trajectory task optimization offline. Thus, a rapid joint trajectory modified method is put forward to suppress vibration of manipulator, which is combination of vibration prediction criteria and three-section DKA modified trajectory. In uncertain tasks, initial joint trajectory is replaced with modified trajectory when vibration is predicted to occur with vibration prediction criteria. Finally, a group of optimal joints trajectory is carried out on manipulator prototype to validate the proposed CP-PSO method and single joint trajectory modified experiment is executed to confirm the rapid joint trajectory modified method.

It is worth mentioning that two factors may affect the practical performance of the proposed CP-PSO: quantity of joint interpolation points and accuracy of dynamic model of manipulator. By increasing computational ability, more joint interpolation points can be sampled. Furthermore, multi joints vibration prediction criteria will be improved to realize manipulator trajectory modified.

ACKNOWLEDGMENT

The authors are great appreciation to the anonymous reviewers for paying their precious time to put forward professional suggestions on improving this manuscript. They also would like to be sincere grateful to Dr. Longzhi Zhang for her valuable suggestion on writing.

REFERENCES

[1] L. M. Sweet and M. C. Good, "Re-definition of the robot motion control problem: Effects of plant dynamics, drive system constraints, and user requirements," in *Proc. IEEE Conf. Decis. Control*, 1984, pp. 724–732.

[2] J. S. Lane and S. L. Dickerson, "Contribution of passive damping to the control of flexible manipulators," in *Proc. Int. Comput. Eng. Conf.*, 1984, pp. 175–180.

[3] T. Liu, Y. Shi, H. Hua, Z. Chen, and X. Shi, "Study on vibration control of thin plate with active constrained layer damping," *J. Mech. Strength*, vol. 24, no. 1, pp. 23–28, 2002.

[4] S. B. Choi, M. V. Gandhi, B. S. Thompson, and C. Y. Lee, "An experimental investigation of an articulating robotic manipulator with a graphite-epoxy composite arm," *J. Field Robot.*, vol. 5, pp. 73–79, Feb. 1988.

[5] D. Bandopadhya, D. K. Bhogadi, B. Bhattacharya, and A. Dutta, "Active vibration suppression of a flexible link using ionic polymer metal composite," in *Proc. IEEE Conf. Robot., Autom. Mechatronics*, Jun. 2006, pp. 1–6.

[6] X. Zhang and Y.-Q. Yu, "Motion control of flexible robot manipulators via optimizing redundant configurations," *Mech. Mach. Theory*, vol. 36, no. 7, pp. 883–892, 2001.

[7] Y. Shigang, "Weak-vibration configurations for flexible robot manipulators with kinematic redundancy," *Mech. Mach. Theory*, vol. 35, no. 2, pp. 165–178, 2000.

[8] M. A. Ahmad, R. M. T. R. Ismail, and M. S. Ramli, "Optimal control with input shaping for input tracking and vibration suppression of a flexible joint manipulator," *Eur. J. Sci. Res.*, vol. 28, no. 4, pp. 583–599, 2009.

[9] S. Kapucu, S. Baysec, and G. Alıcı, "Residual vibration suppression of a flexible joint system using a systematic command shaping technique," *Arabian J. Forence Eng.*, vol. 31, no. 2B, pp. 139–152, 2006.

[10] S. Mahto, "Shape optimization of revolute-jointed single link flexible manipulator for vibration suppression," *Mech. Mach. Theory*, vol. 75, pp. 150–160, May 2014.

[11] H. Deng, J.-D. Sun, S.-D. Huang, and G.-Z. Cao, "Vibration suppression of the flexible manipulator using optimal input shaper and linear quadratic regulator," in *Proc. Int. Conf. Ubiquitous Robots Ambient Intell.*, 2015, pp. 255–260.

[12] R. H. Cannon, Jr., and E. Schmitz, "Initial experiments on the end-point control of a flexible one-link robot," *Int. J. Robot. Res.*, vol. 3, pp. 49–54, Sep. 1984.

[13] M. Ertugrul and O. Kaynak, "Neuro sliding mode control of robotic manipulators," *Mechatronics*, vol. 10, nos. 1–2, pp. 230–263, 2000.

[14] Q. Zhang, J. K. Mills, W. L. Cleghorn, J. Jin, and C. Zhao, "Trajectory tracking and vibration suppression of a 3-PRR parallel manipulator with flexible links," *Multibody Syst. Dyn.*, vol. 33, no. 1, pp. 27–60, 2015.

[15] M. E. Greene and H. Tan, "Indirect adaptive control of a two-link robot arm using regularization neural networks," in *Proc. Int. Conf. Ind. Electron., Control Instrum. (IECON)*, vol. 2, 2001, pp. 952–956.

[16] L. Tian, J. Wang, and Z. Mao, "Constrained motion control of flexible robot manipulators based on recurrent neural networks," *IEEE Trans. Syst., Man, Cybern. B, Cybern.*, vol. 34, no. 3, pp. 1541–1552, Jun. 2004.

[17] T. Zhou, H. Guo, J. Xu, and C. Lin, "Adaptive robust control with input shaping technology for solar array drive system," *Acta Astronaut.*, vol. 140, pp. 264–272, Nov. 2017.

[18] K.-J. Park and Y.-S. Park, "Fourier-based optimal design of a flexible manipulator path to reduce residual vibration of the endpoint," *Robotica*, vol. 11, no. 3, pp. 263–272, 1993.

[19] K.-J. Park, "Flexible robot manipulator path design to reduce the endpoint residual vibration under torque constraints," *J. Sound Vibrat.*, vol. 275, pp. 1051–1068, Aug. 2004.

[20] A. Heidari and A. Nikoobin, "Maximum allowable dynamic load of flexible manipulators with imposing residual vibration constraint," in *Proc. IEEE Int. Conf. Robot. Biomimetics (ROBIO)*, Dec. 2007, pp. 1457–1462.

[21] P. K. Sarkar, M. Yamamoto, and A. Mohri, "Significance of spline curve in path planning of flexible manipulator," in *Proc. IEEE Int. Conf. Robot. Autom.*, vol. 3, Apr. 1997, pp. 2535–2540.

[22] P. K. Sarkar, M. Yamamoto, and A. Mohri, "Sub-optimal trajectory planning of flexible manipulator along specified path," in *Proc. IEEE/RSJ Int. Conf. Intell. Robots Syst.*, vol. 3, Sep. 1997, pp. 1540–1545.

[23] A. Mohri, P. K. Sarkar, and M. Yamamoto, "An efficient motion planning of flexible manipulator along specified path," in *Proc. IEEE Int. Conf. Robot. Autom.*, vol. 2, May 1998, pp. 1104–1109.

[24] R. Béarée, "New Damped-Jerk trajectory for vibration reduction," *Control Eng. Pract.*, vol. 28, pp. 112–120, Jul. 2014.

[25] L. Biagiotti, C. Melchiorri, and L. Moriello, "Optimal trajectories for vibration reduction based on exponential filters," *IEEE Trans. Control Syst. Technol.*, vol. 24, no. 2, pp. 609–622, Mar. 2016.

[26] H. Kojima and T. Kibe, "Optimal trajectory planning of a two-link flexible robot arm based on genetic algorithm for residual vibration reduction," in *Proc. IEEE/RSJ Int. Conf. Intell. Robots Syst.*, vol. 4, Oct./Nov. 2001, pp. 2276–2281.

[27] H. Kojima, A. Morito, K. Konno, and T. Kobayashi, "Residual vibration reduction control after catching a falling steel sphere by a two-link catching flexible robot arm," *Int. J. Appl. Electromagn. Mech.*, vol. 19, nos. 1–4, pp. 361–366, 2004.

[28] W. F. Faris, A. A. Ata, and M. Y. Sa'adeh, "Energy minimization approach for a two-link flexible manipulator," *J. Vib. Control*, vol. 15, pp. 497–526, Feb. 2009.

[29] Y. Shigang, "Redundant robot manipulators with joint and link flexibility—I. Dynamic motion planning for minimum end effector deformation," *Mech. Mach. Theory*, vol. 33, nos. 1–2, pp. 103–113, 1998.
[30] Y. Shigang, "Redundant robot manipulators with joint and link flexibility—II. Residual vibration decreasing," *Mech. Mach. Theory*, vol. 33, nos. 1–2, pp. 115–122, 1998.
[31] S. Yue, D. Henrich, W. L. Xu, and S. K. Tso, "Trajectory planning in joint space for flexible robots with kinematics redundancy," Tech. Rep., 2001.
[32] J. Kennedy and R. Eberhart, "Particle swarm optimization," in *Proc. IEEE Int. Conf. Neural Netw.*, Perth, WA, Australia, vol. 4, Nov./Dec. 2011, pp. 1942–1948.
[33] W. Xu, C. Xu, and D. Meng, "Trajectory planning of vibration suppression for rigid-flexible hybrid manipulator based on PSO algorithm," *Control Decision*, vol. 29, no. 4, pp. 632–638, 2014.
[34] Y. Shi and R. C. Eberhart, "Empirical study of particle swarm optimization," in *Proc. Congr. Evol. Comput. (CEC)*, vol. 3, 1999, pp. 1945–1950.
[35] M. Clerc, "The swarm and the queen: towards a deterministic and adaptive particle swarm optimization," in *Proc. Congr. Evol. Comput. (CEC)*, 1999, pp. 1951–1957.
[36] X. Wei and H. Pan, "The analysis of parameters selection of PSO algorithm for fault diagnosis," in *Proc. Int. Conf. Impuls. Hybrid Dyn. Syst.*, 2007, pp. 2013–2017.
[37] M. Wang, J. Luo, and U. Walter, "Trajectory planning of free-floating space robot using particle swarm optimization (PSO)," *Acta Astronaut.*, vol. 112, pp. 77–88, Jul./Aug. 2015.
[38] P. Xin, J. Rong, Y. Yang, D. Xiang, and Y. Xiang, "Trajectory planning with residual vibration suppression for space manipulator based on particle swarm optimization algorithm," *Adv. Mech. Eng.*, vol. 9, no. 4, pp. 1–16, Apr. 2017.
[39] A. Abe, "Trajectory planning for flexible Cartesian robot manipulator by using artificial neural network: Numerical simulation and experimental verification," *Robotica*, vol. 29, no. 5, pp. 797–804, 2011.
[40] Y.-C. Zhang, M. Chu, H.-X. Sun, and Z.-H. Dong, "Stability control for manipulator space capture by using particle swarm optimization based on distributed controllable dampers," in *Proc. Int. Conf. Autom., Robot. Appl.*, 2015, pp. 574–579.
[41] A. Abe, "Trajectory planning for residual vibration suppression of a two-link rigid-flexible manipulator considering large deformation," *Mech. Mach. Theory*, vol. 44, no. 9, pp. 1627–1639, 2009.
[42] M. W. Spong, "Modeling and control of elastic joint robots," *J. Dyn. Syst., Meas. Control*, vol. 109, no. 4, pp. 310–319, 1987.
[43] B. Siciliano, L. Sciavicco, L. Villani, and G. Oriolo, *Robotics: Modelling, Planning and Control* (Advanced Textbooks in Control & Signal Processing), vol. 4. Springer, 2009, pp. 76–82.

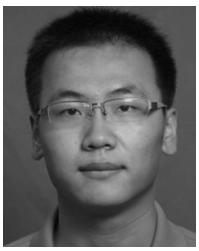

BAOSHI CAO received the B.S. and M.S. degrees in mechatronics engineering from the Harbin Institute of Technology, China, in 2009 and 2012, respectively, where he is currently pursuing the Ph.D. degree with the State Key Laboratory of Robotics and System. His research interests include robotics, trajectory planning of manipulator, and workspace analysis.

KUI SUN received the B.S. degree in mechanization of farming from North-East Agricultural University, Harbin, China, in 1996, and the M.S. and Ph.D. degrees in mechanics from the Harbin Institute of Technology (HIT), Harbin, in 1998 and 2008, respectively. He is currently an Associate Professor with the School of Mechanical Engineering, HIT. His research interests include robotics, inverse kinematics, and dynamics algorithms of a redundant manipulator and its robust control.

TIAN LI received the B.S., M.S., and Ph.D. degrees in mechatronics engineering from the Harbin Institute of Technology (HIT), China, in 2001, 2007, and 2014, respectively. He is currently a Researcher with Beijing Andawell Science & Technology Co., Ltd., China. His research interests focus on the manipulator design, kinematic calibration of manipulator, and robot vibration suppression.

YIKUN GU received the M.S. and Ph.D. degrees in mechatronics engineering from the Harbin Institute of Technology, Harbin, China, in 2006 and 2011, respectively. She is currently an Associate Professor with the School of Mechanical Engineering, HIT. Her research interests include ac motor drives, nonlinear adaptive control, neural networks, and flexible joint robot arm control.

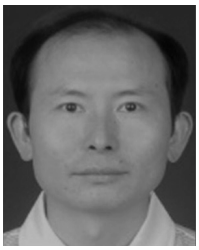

MINGHE JIN received the B.S. degree in vehicle engineering and the M.S. and Ph.D. degrees in mechatronics engineering from the Harbin Institute of Technology (HIT), China, in 1993, 1996, and 2000, respectively. He is currently a Professor with the Robotics Institute, HIT. His research interests include dexterous robot hands, space robotics, and real-time embedded control system.

HONG LIU received the Ph.D. degree from the Harbin Institute of Technology (HIT), China, in 1993. During 1991–1993, he was a Joint Ph.D. Candidate with the Institute of Robotics and System Dynamics, German Aerospace Research Establishment (DLR), Germany, where he has been a Research Fellow since 1993. He became one of the first batches of Changjiang Scholars in 1998. He is currently a Professor with HIT. His research projects include the development of dexterous robot hand and space manipulator.